Incorporating Fluorescent Dyes and Quantum Dots into Magnetic Microbeads for Immunoassays

S. P. Mulvaney, H. Mattoussi, and L. J. Whitman
Naval Research Laboratory
Washington, D.C. 20375

ABSTRACT

Microbeads that are both paramagnetic and fluorescently labeled are commercially available in colors spanning the visible spectrum. Although these commercial beads can be bright, polydispersity in both size and fluorescent intensity limit their use in quantitative assays. Very recently, more monodisperse beads have become available, but their large size and surface properties make them less than ideal for some bioassay applications. Herein, we describe methods to customize commercial, nonfluorescent magnetic microparticles with fluorescent dyes and quantum dots (QDs) without affecting their magnetic or surface chemical properties. Fluorescent dyes and 3.3 nm-diameter CdSe/ZnS QDs were sequestered within 0.8 μm-diameter magnetic beads by swelling the polystyrene matrix of the bead in organic solvent, letting the chromophores partition, and then collapsing the matrix in polar solvents. Chromophore incorporation has been characterized using both uv-visible absorption spectroscopy and fluorescence microscopy, with an average of 3×10^8 rhodamine 6G molecules/bead and 6×10^4 QDs/bead. The modified beads are uniform in size and intensity, with optical properties comparable to currently available commercial beads. Immunoassay results obtained with our custom fluorescent magnetic microbeads are consistent with those obtained using conventional magnetic microbeads.

KEYWORDS: Quantum Dots, Fluorophores, Magnetic beads, Bioassay labels

Address correspondence to : *Dr. L. J. Whitman*
Naval Research Laboratory, Code 6177
Washington, DC 20375-5342 USA
e-mail: whitman@nrl.navy.mil

6 January 2004

INTRODUCTION

Magnetic microbeads are used in a variety of biotechnology applications, most notably for cell sorting and assay separations (1-4). Magnetic microbeads are commercially available from numerous sources, and are commonly composed of iron oxide nanocrystals embedded within a spherical polystyrene matrix. Beads can be readily purchased with a variety of biocompatible surface terminations, such as $-CH_3$, $-NH_2$, or -COOH, that are suitable for further conjugation with functional biochemical ligands and receptors (e.g., antibodies and oligonucleotides).

Recently magnetic beads have been adapted as labels for biochemical binding assays with a variety of detection schemes (5-12). For example, giant magnetoresistive (GMR) (8-15) and Hall sensors (16,17) are two magneto-electronic devices that can be used to sense the weak magnetic fields generated by a magnetic microbead. Although such devices can be sensitive to single beads, the sensors are complicated to fabricate, and their use for quantitative detection requires magnetically monodispersed beads.

Alternatively, optical detection of microbead labels can be an off-the-shelf approach to reading the results of binding assays. The Naval Research Laboratory has been developing a highly specific and sensitive biosensor system using magnetic immunobeads as both optically-detected reporter labels and as transducers for magnetic force discrimination (10). In the Force Discrimination Biosensor (FDB) system, capture antibodies (Abs) are immobilized on a transparent substrate. The sample is then introduced, and analyte specific to the Ab is captured. Magnetic microbeads functionalized with secondary Abs specific to a different epitope on the analyte are then introduced to complete labeling of the captured antigen. Finally, a magnetic force is applied that is too weak to rupture the immunochemical complexes, but strong enough to remove beads bound to the substrate by nonspecific interactions (18). The concentration of the

analyte is determined by optically recording the fraction of beads retained on the substrate following magnetic force discrimination. For ~1 μm-diameter beads, off-the-shelf microscopy components (e.g. an inverted optical microscope and frame grabbing software) can be used for rapid image acquisition and bead counting.

Although quantitative assays using magnetic microbead labels can be performed by particle counting using off-the-shelf optics, a relatively expensive objective is required to achieve sufficient magnification and resolution for beads ~1 μm in diameter. One solution to this limitation would be the use of fluorescent magnetic beads, which would enable individual beads to be imaged with lower-magnification optics, and offer the potential for photon-counting that would not require resolving individual beads. In general, the addition of fluorescence should be useful in applications employing sub-micron magnetic particles, enabling routine detection with optical systems commonly available in biochemistry laboratories. Unfortunately, to our knowledge, there are few commercial sources of beads that are both fluorescent and magnetic. Although such commercial beads are generally bright and available with fluorophores spanning the visible spectrum, we have found them to be too polydisperse in both size and fluorescent intensity to use in quantitative assays. Very recently, more monodisperse fluorescent beads have become available, but their large size and high nonspecific binding with our substrates make them less than ideal for our immunoassay applications.

Herein we describe methods to load commercial magnetic microbeads with fluorophores and quantum dots. We have successfully entrapped several fluorescent dyes and 3.3 nm-diameter quantum dots in SeraMag® beads—relatively monodisperse, 0.8 μm-diameter paramagnetic particles. We compare the properties of the different chromophore loaded beads and investigate their use as labels in a sandwich immunoassay.

MATERIALS AND METHODS

SeraMag® beads, 0.8 μm in diameter, were obtained from Seradyn (Indianapolis, IN, USA). Encapsulated magnetic microbeads loaded with Dragon Green dye (#L010212B) and Compel™ beads, 8.4 μm in diameter, loaded with Dragon Green dye (#030516A) were purchased from Bangs Labratories (Fisher, IN, USA). For the remainder of the paper the beads are referred to as follows: '**S**' for SeraMag beads, '**B1**' for Bang's encapsulated magnetic microbeads, and '**B2**' for Bang's Compel microbeads. CH_2Cl_2, CH_3OH, and CH_3CH_2OH were purchased from Fisher (Houston, TX, USA), rhodamine 6G (R6G) and coumarin 334 from Aldrich (Milwaukee, WI, USA), Alexa Fluor® 568 from Molecular Probes (Eugene, OR, USA), and europium (III) thenoyltrifluoroacetonate trihydrate from Acros (Geel, Belgium). CdSe/ZnS quantum dots (QDs) 3.3 nm in diameter and capped with trioctylphosphine oxide (TOPO) were prepared as previously described (with an expected quantum yield of 40–60%) (19,20).

S beads were washed with CH_3CH_2OH five times in a ratio of 500 μL beads:2 mL CH_3CH_2OH, using magnetic retention during exchange of the CH_3CH_2OH aliquots. The beads were then resuspended in CH_3CH_2OH and stored at 4° C. Prior to chromophore incorporation, washed beads were sonicated for 10 min. to resuspend. Fluorescent dye (e.g., 16.7 mM R6G) was dissolved in CH_2Cl_2, and 500 μL each of washed beads, dye solution, and CH_2Cl_2 were mixed in a 1.5 mL microfuge tube. The tube was capped, placed in a Styrofoam microfuge tube holder, and shaken on a Vortex Genie for 1 hr. The beads were magnetically retained in the tube while the supernatant was removed (and saved for analysis). Finally, the beads were washed three times in CH_3OH, twice in H_2O, and stored at 4° C.

QD entrapment was achieved in a similar manner for the fluorescent dyes using a slightly different reagent mixture. Because TOPO-capped QDs flocculate in the presence of CH_3CH_2OH

(19,20), the CH_3CH_2OH was first removed from a 200 μL bead sample and the beads re-suspended in 200 μL of CH_2Cl_2. This bead solution was then mixed in a microfuge tube with 1000 μL of 2 μM QDs in CH_2Cl_2. The process continued via shaking as described above.

Optical micrographs were collected on an inverted Zeiss Axiovert® 100 microscope (Gottingen, Germany) in either transmission mode or fluorescence using a Hg lamp and Zeiss filter sets #2 (for QDs: excitation 365 nm, emission LP420 nm), #5 (for coumarin 334 and Dragon Green: ex. 395-440 nm, em. LP470 nm), #10 (for coumarin 334 and Dragon Green: ex. 450-490 nm, em. 515-565 nm), and #14 (for R6G: ex. 510-560 nm, em. LP590 nm). Images were collected with a Roper Scientific CoolSNAP-PRO*cf*® thermally-cooled, monochrome CCD camera (Trenton, NJ, USA).

RESULTS AND DISCUSSION

S beads are core-shell particles made with a polystyrene core, a layer of maghemite nanocrystals, and an outer shell of polystyrene. Our methodology for incorporating fluorescent dyes and QDs into the beads is adapted from literature reports of fluorescent dye entrapment in polymer matrices (21-23). As discussed in these reports, these methods physically sequester the chromophore within the matrix. In our case, encapsulation is achieved by swelling the polystyrene bead matrix in an organic solvent (often CH_2Cl_2), letting the chromophores partition into the polystyrene, and then collapsing the swollen bead in polar solvents (CH_3OH, followed by H_2O). The chromophores are thereby trapped inside the polystyrene beads; no detectable leaching has been observed. An advantage of this approach is that the bead surface chemistry is nominally unaffected, remaining amenable to further functionalization for binding assays.

Transmission and fluorescent gray-scale micrographs of **S** beads encapsulated with R6G, coumarin 334, or QDs are displayed in Figure 1; for comparison, commercial beads that are both

fluorescent and magnetic are also shown. Bead lots with uniform luminescence can be made from each of the chromophores, but the intensity of the luminescent signal per bead varies depending on the chromophore's affinity for the polystyrene matrix and the solvent used. It is important to note that photobleaching occurs for dye-loaded beads; for example, R6G beads photobleach after 15 min of continuous excitation with a Hg lamp (5 mW power at sample).

Uniform luminescence is a key criterion for the custom beads to be suitable for use as immunoassay labels. We have characterized the chromophore loading levels using both uv-visible absorption spectroscopy and fluorescence microscopy. The absolute amount of dye entrapped per bead lot can be determined by comparing the absorbance of each dye solution before and after the encapsulation procedure and calculating the concentration-dependence of the absorbance as follows. For R6G, the absorbance (A) of four known concentrations (C, in μM) was measured and fit linearly ($R^2 = 0.99$),

$$A = (0.128\ \mu M^{-1})C - 0.007\ . \qquad (1)$$

The number of molecules entrapped can then be calculated from the total volume of each sample (1.5 mL) and its dilution. Beads incorporating R6G were the brightest beads made, with an average of 3×10^8 R6G molecules/bead, as detailed in Table 1.

The absolute number of beads present in a sample volume can be calculated based on the fraction of each bead composed of magnetic material (40% by volume), and the starting bead concentration (50 mg/mL) (http://www.seradyn.com). If 40% of the bead volume is maghemite (4.9 g/cm^3) and 60% is polystyrene (1.05 g/cm^3), then each 0.8 μm-diameter bead should weigh 6.93×10^{-13} g. Our protocol uses 500 μL of beads washed in CH_3CH_2OH, corresponding to a bead concentration of 12.5 mg/mL, or 9.02×10^9 beads per lot. Using the absolute amount of chromophore entrapped per bead lot, the average chromophore loading per bead can therefore be

determined (Table 1). Note that bead retention during the washing steps is not perfect, so the estimated number of beads per sample represents an upper bound. Furthermore, the uv-visible spectroscopy is done with small volumes of organic solvent and there is uncertainty associated with the accuracy and reproducibility of pipeting these liquids; overall, we estimate the uncertainty of the loading to be 15%.

The quantity of QDs incorporated into the beads can be estimated in an analogous manner utilizing the absorbance peak at 230 nm, with the resulting linear calibration,

$$A = (0.0092\ \mathrm{nM}^{-1})C + 0.0474\ . \qquad (2)$$

In this case, each sample started with a 200 μL aliquot of washed bead solution (12.5 mg/mL) and a total reaction volume of 1100 μL. As detailed in Table 2, an average of 69,000 QDs was incorporated in each bead. The lower number of QDs incorporated per bead compared with R6G molecules is not surprising given their much larger size.

Although the analysis of chromophore solutions by absorption spectroscopy demonstrates that consistent average loading levels per bead lot can be achieved, it does not indicate the level of uniformity among beads within a lot. Therefore, individual beads were characterized by dispersing them on a glass slide and collecting the fluorescence signal with a CCD camera. The brightness of each bead was recorded as the 8-bit pixel intensity (0–255) after subtracting the local background. Comparisons were made between **S** beads labeled with R6G and QDs, and commercial fluorescent-magnetic microbeads (**B1**, **B2**). As shown in Figure 2, the **S**-R6G loaded beads are typically 2 times more uniform than ones incorporating QDs. Compared to the **B1** beads, the **S**-R6G and **S**-QD beads are about 4 and 2 times more uniform, respectively.

Figure 2 also shows differences in the average raw intensity of each bead type, suggesting overall differences in brightness. However, the total amount of light emitted from each bead

depends on a number of factors, including the total amount of chromophore incorporated (a function of the bead size), the absorption coefficient of the chromophore, and the quantum yield of the chromophore. In practice, however, the optical characteristics of magnetic beads made as we describe is more likely to depend on the bead size, bead surface chemistry, and instrumentation requirements for the assay rather than on the optical physics. A full exploration of all the factors that affect bead brightness is beyond the scope of this work.

The difference in brightness and uniform intensity of the **B1** beads compared with the two types of **S** beads can be partially explained by the relative polydispersity in their size. Based on optical micrographs, the average diameter of the **B1** beads was 2.19 ± 0.98 μm compared with 0.80 ± 0.12 μm for the **S** beads (Figure 3). **B2** beads have recently become available and address some of the shortcomings of the **B1** beads related to polydispersity. This new class of bead is currently available in three diameters, 2.7, 6.0, and 8.4 μm, with the 8.4 μm bead available labeled with Dragon Green dye. These dyed beads show better monodispersity in size and intensity (Figures 2 and 3) than both **S** and **B1** beads. However, the extremely large size of the **B2** beads and their high nonspecific binding with our substrates make them unsuitable for use in FDB immunoassays (data not shown).

To confirm that our chromophore incorporation process is compatible with the subsequent functionalization and use, we have conjugated the **S**-R6G beads with Abs (for *Bacillius anthracis*) and used them for a FDB sandwich immunoassay (10). As illustrated in Figure 4, the microbead labels bind to target (sonicated *Bacillius anthracis* spores, 10^3 cfu/ml) captured onto the functionalized substrate. The distinguishing feature of this assay is that a magnetic force is then applied to remove beads bound to the substrate by weak, non-specific interactions, reducing assay background and thereby increasing both the sensitivity and specificity of the assay. By

comparing fluorescent optical micrographs of the substrate before and after application of the discriminating force (Figure 4B,D and 4C,E, respectively), the fraction of the beads retained—proportional to the target concentration—can be determined. Note that we have not observed any qualitative change in the response of chromophore-modified beads to the magnetic field gradient used for force discrimination, indicating the modification chemistry does not lead to appreciable loss of magnetic material. Assay results obtained with the fluorescent microbeads are consistent with those obtained with conventional beads using transmission microscopy (Figure 4E, INSET). In this case, the fraction of beads retained above background with fluorescent beads was 16 ± 3% versus 20 ± 3% with the original beads. Although these experiments were all performed with high-magnification optics, the ease of using fluorescence to identify beads demonstrates the feasibility of using a lower magnification optical system for bead detection. (We are currently fabricating such a system.)

In conclusion, the ability to use magnetic microbeads for both separation and detection makes them a valuable tool for a wide range of biotechnology applications. The addition of fluorescence to magnetic microbeads not only simplifies their optical detection, but offers additional multiplexing and "bar-coding" possibilities. Commercial sources exist that provide beads that are both fluorescent and magnetic, but limitations exist in homogeneity, fluorescent dyes incorporated, and bead sizes available. We have described a simple method to custom modify polystyrene-based magnetic microbeads to give uniform fluorescence signatures without affecting the magnetic or surface chemical properties. We have found that a variety of chromophores spanning the visible spectrum can be incorporated into submicron diameter particles, with R6G producing our best beads. The chromophores are physically entrapped within the polystyrene matrix, with no evidence of leaching. This general method should give

researchers flexibility to fluorescently customize whichever magnetic microbeads are best for their applications.

ACKNOWLEDGEMENTS

We are grateful to Christina Cole and Alicia Scribner for their assistance with the immunoassays. This work was supported by the Office of Naval Research and the Joint Science and Technology Panel for Chemical Biological Defense through the U.S. Army. SPM would also like to acknowledge the National Research Council Research Associateship Program.

REFERENCES

1. **Melville, D., Paul, F., Roath, S.** 1975. Direct magnetic separation of red-cells from whole blood. Nature. *255*:706.
2. **Patolsky, F., Weizmann, Y., Katz, E., Willner, I.** 2003. Magnetically amplified DNA assays (MADA): sensing of viral DNA and single-base mismatches by using nucleic acid modified magnetic particles. Angew. Chem. Int. Ed. *42*:2372-2376.
3. **Choi, J.-W., Liakopoulous, T.M., Ahn, C. H.** 2001. An on-chip magnetic bead separator using spiral electromagnets with semi-encapsulated permalloy. Biosens. Bioelectron. *16*:409-416.
4. **Choi, J.-W., Ahn, C.H., Bhansali, S., Henderson, H.T.** 2000. A new magnetic bead-based, filterless bio-separator with planar electromagnet surfaces for integrated bio-detection systems. Sens. Actuat. B-Chem. *68*:34-39.
5. **Weizmann, Y., Patolshi, F., Katz, E., Willner, I.** 2003. Amplified sensing and immunosensing by the rotation of functional magnetic particles. J. Am. Chem. Soc. *125*:3452-3454.
6. **Richardson, J., Hawkins, P., Luxton, R.** 2001. The use of coated paramagnetic particles as a physical label in a magneto-immunoassay. Biosens. Bioelectron. *16*:989-993.
7. **Richardson, J., Hill, A., Luxton, R., Hawkins, P.** 2001. A novel measuring system for the determination of paramagnetic particle labels for use in magneto-immunoassays. Biosens. Bioelectron. *16*:1127-1132.

8. **Baselt D.R., Lee, G.U., Natesan, M., Metzger, S.W., Sheehan, P.E., Colton, R.J.** 1998. A biosensor based on magnetoresistance technology. Biosens. Bioelectron. *13*:731-739.

9. **Edelstein, R.L., Tamanaha, C.R., Sheehan, P.E., Miller, M.M., Baselt, D.R., Whitman, L.J., Colton, R.J.** 2000. The BARC biosensor applied to the detection of biological warfare agents. Biosens. Bioelectron. *14*:805-813.

10. **Lee, G.U., Metzger, S., Natesan, M., Yanavich, C., Dufrêne, Y.F.** 2000. Implementation of force differentiation in the immunoassay. Anal. Biochem. *287*:261-271.

11. **Rife, J.C., Miller, M.M., Sheehan, P.E., Tamanaha, Tondra, M., Whitman, L.J.** 2003. Design and performance of GMR sensors for the detection of magnetic microbeads in biosensors. Sens. Actuat. A-Phys. *107*:209-218.

12. **Baselt, D.R., Lee, G.U., Colton, R.J.** 1996. Biosensor based on force microscope technology. J. Vac. Sci. Technol. B *14*:789-793.

13. **Cziraki, A., Koteles, M., Peter, L., Kupay, J., Padar, J., Pogany, L., Bakonyi, I., Uhlemann, M., Herrich, M., Arnold, B., Thomas, J., Bauer, H.D., Wetzig, K.** 2003. Correlation between interface structure and giant magnetoresistance in electrodeposited Co-Cu/Cu multilayers. Thin Solid Films *433*:237-242.

14. **Luby, S., Majkova, E., Debnarova, A., Senderak, R., Ac, V., Anwarzai, B.** 2003. Effect of magnetic flux distribution on GMR in Ag/Co multilayers. Thin Solid Films *433*:243-246.

15. **Pattanaik, G.R., Pandya, D.K., Kashyap, S.C.** 2003. Effect of process parameters on GMR in electrodeposited Cu-Co nanogranular thin films. Thin Solid Films *433*:247-251.

16. **Rahm, M., Raabe, J., Pulwey, R., Biberger, J., Wegscheider, W., Weiss, D., Meier, C.** 2002. Planar hall sensors for micro-hall magnetometry. J. Appl. Phys. *91*:7980-7982.

17. **Johnson, M.** 1998. Hybrid ferromagnetic-semiconductor devices. J. Vac. Sci. Technol. A *16*:1806-1811.

18. **Lee, G.U., Chrisey, L.A., Colton, R.J.** 1994. Direct measurement of the forces between complementary strands of DNA. Science *266*:771-773.

19. **Mattoussi, H., Mauro, J.M., Goldman, E.R., Anderson, G.P., Sundar, V.C., Mikulec, F.V., Bawendi, M.G.** 2000. Self-assembly of CdSe-ZnS quantum dot bioconjugates using an engineered recombinant protein. J. Am. Chem. Soc. *122*:12142-12150.

20. **Mattoussi, H., Mauro, J.M., Goldman, E.R., Green, T.M., Anderson, G.P., Sundar, V.C., Bawendi, M.G.** 2001. Bioconjugation of highly luminescent colloidal CdSe-ZnS quantum dots with an engineered two-domain recombinant protein. Phys. Stat. Sol. B *224*:277-283.

21. **Levitus, M., Bourdelande, J.L., Marques, G., Armendia, P.F.** 1999. Fluorescence anisotropy of dyes included in crosslinked polystyrene. J. Photochem. Photbiol. A-Chem. *126*:77-82.

22. **Tauer, K., Kaspar, H., Antonietti, M.** 2000. Equilibrium swelling of colloidal polymeric particles with water-insoluble organic solvents. Colloid Polym. Sci. *278*:814-820.

23. **Han, M., Gao, X., Su, J.Z., Nie, S.** 2001. Quantum-dot-tagged microbeads for multiplexed optical coding of biomolecules. Nat. Biotechnol. *19*:631-635.

TABLE LEGENDS

Table 1. Rhodamine 6G incorporation into **S** beads.

Table 2. CdSe/ZnS quantum dot (QD) incorporation into **S** beads.

FIGURE LEGENDS

Figure 1. Transmission and fluorescence optical micrographs of S beads after incorporation of chromophores. Transmission are shown on the left, and fluorescence on the right for R6G (A,B), coumarin 334 (C,D), and QDs (E,F). For comparison, commercial beads that incorporate Dragon Green are also shown: **B1** (G,H) and **B2** (I,J). Micrographs were taken with a 100x, 1.3 Plan-NEOFLUAR® objective. Note that because of the small depth of field at this magnification, there is some variance in the apparent size of the beads caused by variance in the focal plane with respect to the center of each bead.

Figure 2. Histograms of the intensity distributions among different fluorescent, magnetic microbeads.

Figure 3. Histograms of the size distributions among different fluorescent, magnetic microbeads.

Figure 4. The use of fluorescently-modified S beads in a magnetic force discrimination immunoassay. (A) Schematic illustration of the assay (not to scale). (B-E) Fluorescence micrographs ($128 \times 96\ \mu m^2$) of the substrate before and after application of the discriminating force, respectively, showing the detection of (B,C) 0 cfu/mL and (D,E) 10^3 cfu/mL *Bacillius anthracis*. The image INSET in E is from a comparable assay performed with conventional beads using transmission microscopy.

	Starting R6G Solution			Recovered Dye Solution			Amt. of Dye	R6G molecules
Trial	Abs. (527 nm)	Conc. (μM)	Dilution adjust (mM)	Abs. (527 nm)	Conc. (μM)	Dilution adjust (mM)	Retained (mM)	per bead ($x10^8$)
1	0.962	7.57	5.68	0.446	3.54	2.65	3.03	3.03
2				0.376	2.99	2.24	3.44	3.45
3	0.922	7.26	5.44	0.322	2.57	1.93	3.51	3.52
4				0.351	2.80	2.10	3.34	3.34
5				0.399	3.17	2.38	3.06	3.06
6				0.290	2.32	1.74	3.70	3.71
Avg	0.942			0.364				3.35
St. Dev.	0.028			0.056				0.27

Mulvaney *et al.* "Incorporating Fluorescent Dyes…", Table 1.

	Starting QDs Solution			Recovered QDsSolution			# of QDs	QDs per
Trial	Abs. (230 nm)	Conc. (nM)	Dilution adjust (μM)	Abs. (230 nm)	Conc. (nM)	Dilution adjust (μM)	Retained ($x10^{14}$)	bead ($x10^{4}$)
1	0.657	66.3	2.05	0.437	42.4	1.61	3.30	9.16
2	0.664	67.0	2.08	0.445	43.2	1.64	2.92	6.85
3	0.613	61.5	1.91	0.449	43.7	1.65	1.67	4.63
Avg	0.645			0.444				6.88
St. Dev.	0.028			0.006				2.27

Mulvaney *et al.* "Incorporating Fluorescent Dyes…",Table 2.

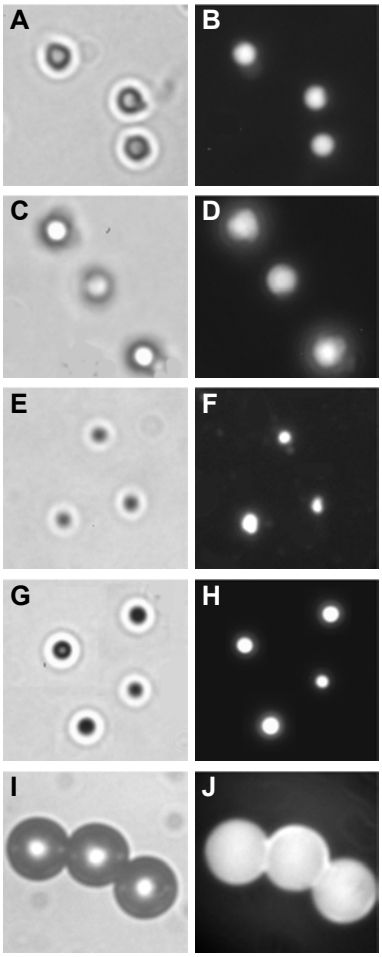

Mulvaney *et al.* “Incorporating Fluorescent Dyes…”, Figure 1.

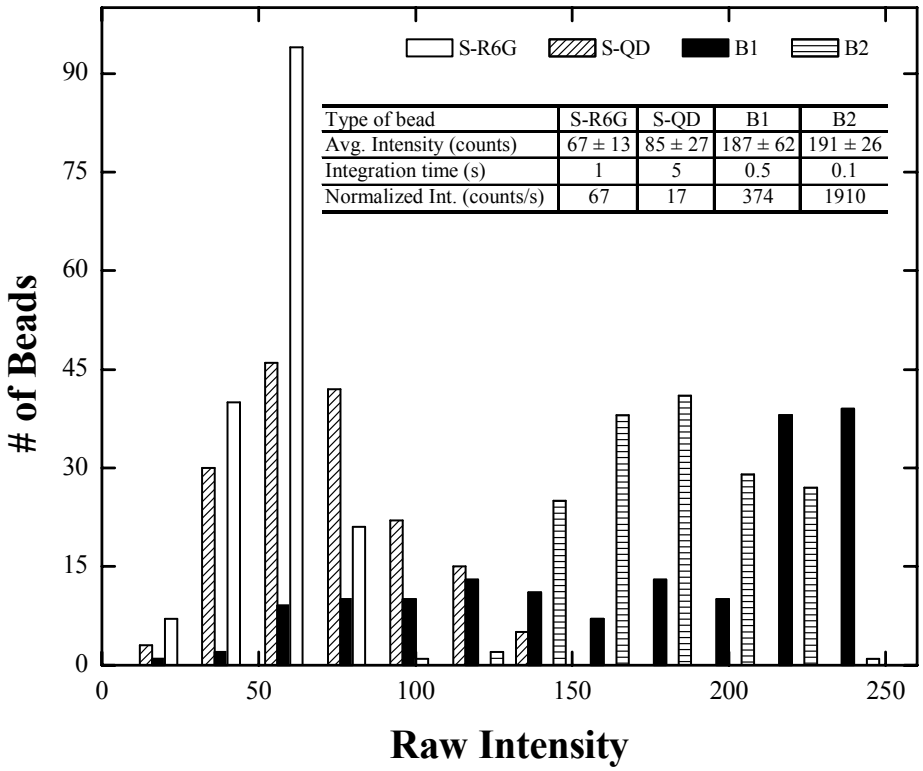

Type of bead	S-R6G	S-QD	B1	B2
Avg. Intensity (counts)	67 ± 13	85 ± 27	187 ± 62	191 ± 26
Integration time (s)	1	5	0.5	0.1
Normalized Int. (counts/s)	67	17	374	1910

Mulvaney *et al.* "Incorporating Fluorescent Dyes…", Figure 2.

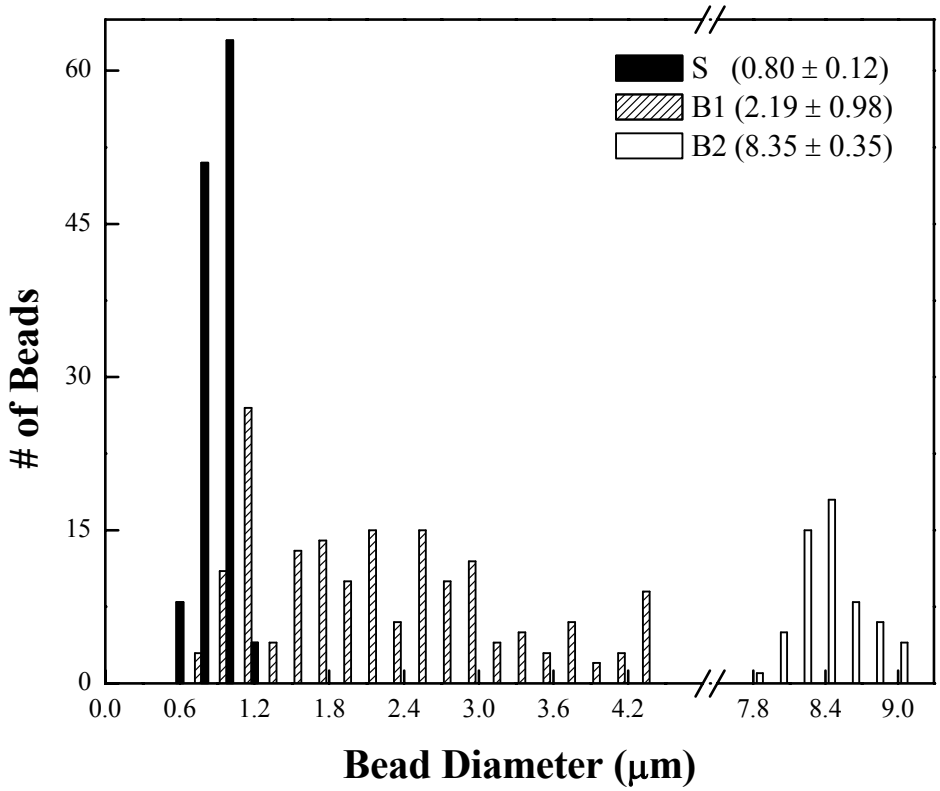

Mulvaney *et al.* "Incorporating Fluorescent Dyes…", Figure 3.

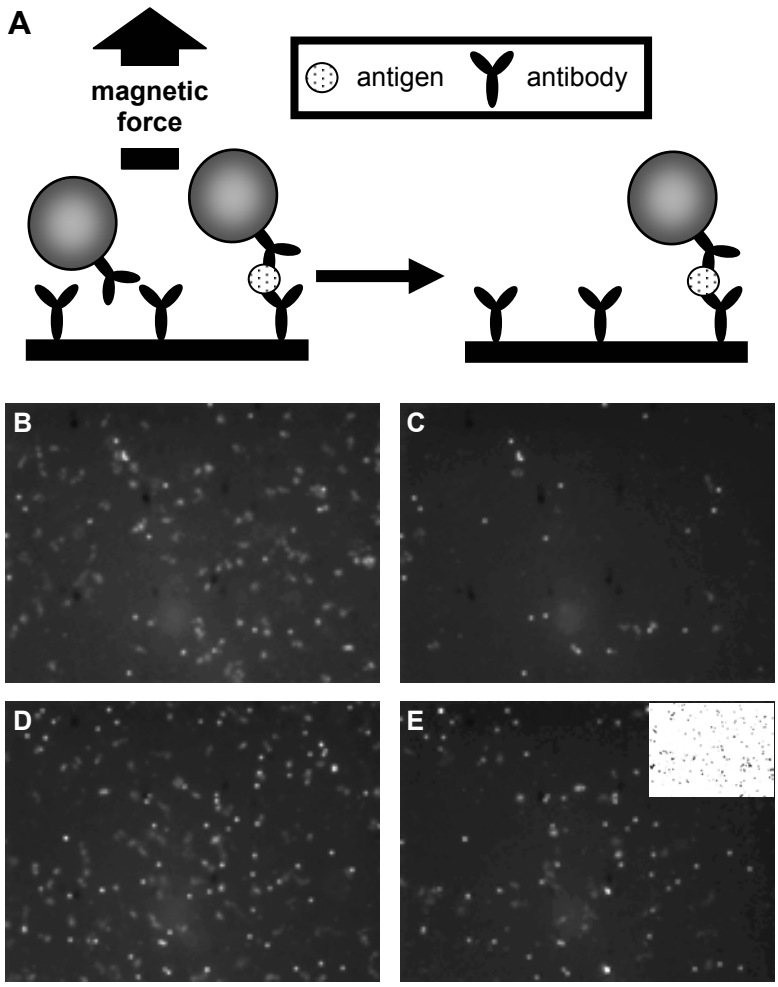

Mulvaney *et al.* "Incorporating Fluorescent Dyes…", Figure 4.